

EVAPORATION OF SPINEL-RICH CAI MELTS: A POSSIBLE LINK TO CH-CB CAIs. M. A. Ivanova^{1,2}, R. A. Mendybaev³, S. I. Shornikov¹, K. M. Ryazantsev¹, and G. J. MacPherson². ¹Vernadsky Institute, Kosygin St. 19, Moscow 119991 (meteorite2000@mail.ru); ²Department of Mineral Sciences, National Museum of Natural History, Smithsonian Institution, Washington, DC 20560; ³University of Chicago, Chicago, IL 60637.

Introduction: The most important processes in formation of calcium-aluminum inclusions (CAIs) were condensation, melting and evaporation. The bulk compositions of CAIs record the cumulative effects of these high-temperature and largely volatility-controlled processes during the first several million years of solar system history [1]. We recently presented results on thermodynamic modeling of evaporation of CAIs with different compositions from CV3 chondrites, and compared their evaporation trends with the bulk compositions of CAIs from CV3 and CH-CB chondrites [2]. The calculations showed that unlike for most other CAI composition melts, evaporation of a melt with a spinel-rich and calcium-poor CAI composition (5aN) starts with faster evaporation of Si over Mg, resulting in a compositional trend that well fits the CAI compositions of CH-CB chondrites [2]. Unlike most CAIs from CV chondrites, 5aN is a pristine fine-grained spinel-rich inclusion with no traces of melting or evaporation. Its Al₂O₃-enriched bulk composition has a non-solar CaO/Al₂O₃ ratio of ~0.3. The bulk chemical composition of 5aN is plotted in the anorthite field of spinel-rich CAIs on a Ca₂SiO₄-Al₂O₃-Mg₂SiO₄ diagram [2].

Here we report experimental results on the evaporation of a CAI 5aN-like composition and compare them with thermodynamic calculations. The results are used to investigate the evolution of the bulk chemical composition of 5aN during evaporation and to check if 5aN-like CAIs could serve as precursors of CAIs in CH-CB chondrites.

Experimental and analytical methods: As a starting material in the experiments we used a CAI 5aN-like composition prepared by mixing MgO, SiO₂, Al₂O₃ and CaCO₃ with CaO/Al₂O₃ ratio of ~0.3. The composition was evaporated in a vacuum furnace at 1900°C for 0 to 45 minutes (Table 1) at total pressure ~10⁻⁶ torr using experimental procedures per [4, 5]. One run (“5aN-3”) was quenched as soon as the furnace temperature have reached 1900°C; its analyzed composition is taken as the starting composition in all our experiments. Texture and chemical composition of the evaporation residues were studied at the University of Chicago using TESCAN LYRA3 FIB/FESEM equipped with an Oxford AZtec x-ray microanalysis system, and at the Smithsonian Institution using a FEI NOVA NanoSEM 600 SEM (EDS) and JEOL 8530F Hyperprobe (WDS). Mineral chemistry of evaporated

residues was also performed by JEOL 8530F Hyperprobe.

Results: The typical textures of the 5aN experimental residues are shown in Fig.1. Most of the run products (Fig. 1a) consist of intergrowths of quench textured “Christmas tree”-like spinel and glass. The most evaporated samples 5aN-1 and 5aN-7 which lost all its MgO and SiO₂ (Table 1) are composed mostly of hibonite and CaAl₂O₄ with a minor amount of CaAl₄O₇ (Fig. 1b). It is interesting to note that as evaporation proceeds spinel gradually becomes more saturated in Al₂O₃ compared to the stoichiometric one.

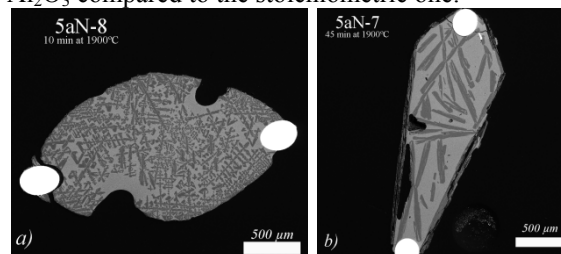


Fig. 1. Backscattered electron images of the experimental residues: a) typical texture with “Christmas tree”-like spinel (dark) and glass (light); b) texture of most evaporated residues with hibonite (dark) and CaAl₂O₄ (light).

Table 1. Bulk compositions of evaporated samples

sample	time, min	MgO, wt%	Al ₂ O ₃ , wt%	SiO ₂ , wt%	CaO, wt%	CaO / Al ₂ O ₃	% Mg lost	% Si lost
5aN-3	0	16.02	37.72	33.71	12.56	0.33	0.0	0.0
5aN-6	5	15.77	43.07	27.17	14.00	0.33	13.8	29.4
5aN-8	10	14.46	46.07	23.91	15.56	0.34	26.1	41.9
5aN-5	15	12.69	50.59	19.87	16.85	0.33	41.0	56.0
5aN-2	15	11.43	57.63	13.95	16.99	0.29	53.3	72.9
5aN-4	25	6.49	63.62	9.11	20.79	0.33	76.0	84.0
5aN-1	30	0.01	76.88	0.09	23.02	0.30	100.0	99.9
5aN-7	45	0.00	76.66	0.05	23.29	0.30	100.0	99.9

% Mg and % Si lost have been calculated relative to 5aN-3 (0 min run) chemical compositions of which has been considered as a starting composition of the samples before evaporation at 1900 °C

Bulk compositions of experimental run products of 5aN are presented in Table 1 and plotted on a Ca₂SiO₄-Al₂O₃-Mg₂SiO₄ diagram (Fig. 2). The diagram also shows the calculated evaporation trajectory of CAI 5aN as well as available experimental evaporation trajectories of CAIB [5] and CAI4 [6] melts with bulk compositions somewhat close to that of 5aN.

As refractory Ca and Al do not evaporate under conditions of the experiments (CaO/Al₂O₃ ratio in evaporation residues would remain constant until all Si and Mg are lost), the weight loss of samples is caused by evaporation of Mg and Si. Fig. 3 shows the experimental evaporation trajectories for 5aN along with

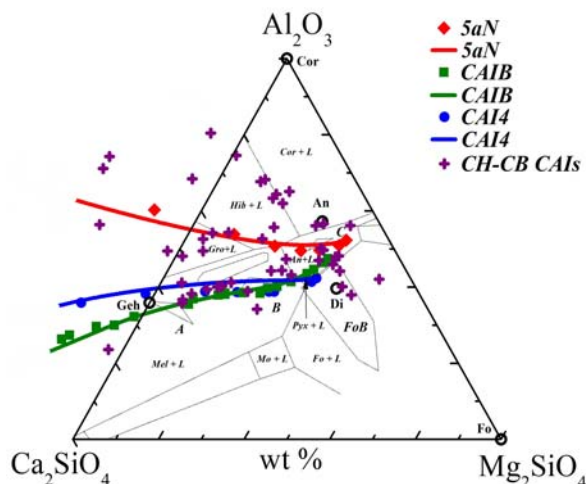


Fig. 2. Experimental (lines) and calculated (symbols) compositional trends of CAIs material: *5aN*, *CAI4* and *CAIB* evaporation compare to CH-CB CAIs bulk compositions.

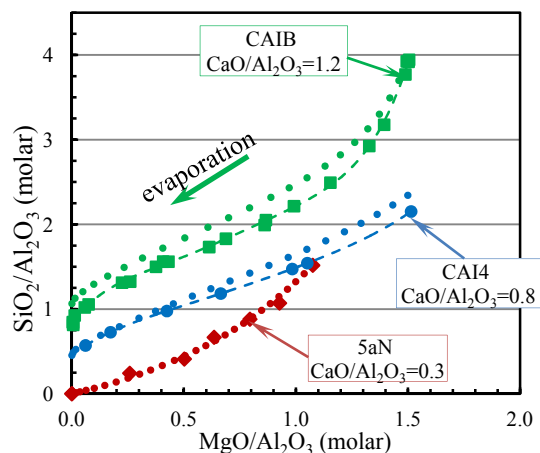


Fig. 3. Experimental trajectories for *5aN*, *CAIB* [5] and *CAI4* [6] melts evaporated at 1900 °C in vacuum. Dots are thermodynamic calculations; dashed lines are best fits to the experimental data. Starting composition of *CAI4* used in the calculations contained 1 wt% more SiO_2 , and 0.5 wt% less Al_2O_3 than the composition used in the experiments.

those for *CAIB* [5] and *CAI4* [6], and the thermodynamically calculated trajectory for *5aN* melt. First, note good agreement between calculated and experimentally determined trends. Second, evaporation of *5aN* starts with much faster loss of Si compared to Mg, which is similar to the initial *CAIB* trend. This might be due to the fact that the initial chemical compositions of both *5aN* and *CAIB* melts are plotted in anorthite stability field in Fig. 2. As evaporation proceeds, the rates of Si and Mg loss become comparable, and in highly processed *5aN* melt Mg evaporates faster than Si and the trend shifts toward Ca-aluminates. In case of evaporation of more SiO_2 -rich and MgO-poor *CAIB*

melt with $\text{CaO}/\text{Al}_2\text{O}_3=1.2$, the residual melt evolves toward gehlenite-rich melilite.

Unlike our *5aN* and *CAIB* melts, an initial faster loss of Mg compared to Si was observed when MgO-rich forsteritic melts were evaporated in vacuum [4, 7] and in thermodynamically calculated trends for several CAIs from CV chondrites [2, 3, 9]. Note also the different evaporation trajectories of *5aN* and *CAI4* melts with the same $\text{MgO}/\text{Al}_2\text{O}_3$ and $\text{SiO}_2/\text{Al}_2\text{O}_3$ ratios (~ 1.1 and ~ 1.5 correspondingly, where *5aN* and *CAI4* curves intersect in Fig. 3), yet different $\text{CaO}/\text{Al}_2\text{O}_3$. Taken together, these differences in evaporation trajectories are most likely due to the difference in starting melt compositions. This suggests that melt structure plays an important role during the evaporation process.

Discussion. As shown on Fig. 2, the compositional trends of evaporated *5aN*, *CAIB* and *CAI4* melts obtained in experiments and by theoretical model calculations are very similar. The experiments confirm our thermodynamic calculations based on the theory of associated solutions and on experimental data for activities of oxides in the system $\text{CaO-MgO-FeO-Al}_2\text{O}_3\text{-TiO}_2\text{-SiO}_2$ [3,8]. Both experiments and calculations show that evaporation of CAI *5aN*-like melt results in a compositional trend that well fits the CAI compositions of CH-CB chondrites [2] (Fig. 2). The reason why the evaporative trend of *5aN*-like melt is different from those with other compositions studied (like *CAIB* or *CAI4*) is not clear: it might be due to the melt composition being in the anorthite stability field with high concentrations of Al_2O_3 ; or is caused by acidity-basicity factors of the melts [10].

Our results showed that spinel-rich melts can be possible precursors for very refractory population of CAIs from CH-CB chondrites. If so, they should show fractionated isotopic effects in Mg and O, but CAIs from CH-CBs didn't record such the effect [11]. Lack of isotopic signatures can be explained by melting of the precursors under relatively high-pressure conditions. Further isotopic investigations may help to resolve this problem.

References: [1] MacPherson G. J. (2014) *Treatise on Geochemistry* (second edition), 1 (Ed. A. M. Davis) 139–179. [2] Ivanova M. A. et al. (2017) *LPS XLVIII*, Abs. #1363. [3] Shornikov S. I. et al. (2017) *LPS XLVIII*, Abs. #1964. [4] Mendybaev R. A. et al. (2013) *GCA*, 123, 368–384. [5] Richter F. M. et al. (2007) *GCA*, 71, 5544–5564. [6] Mendybaev R. A. and Richter F. M. (2016) *LPS XLVII*, Abs. #2929. [7] Mendybaev et al. (2014) *LPS XLV*, Abs. #2782. [8] Shornikov S. I. et al. (2015) *International Conf. XVI, Physico-chemistry and Petrology in the Earth Sciences*, 281–284. [9] Ivanova M. A. et al. (2016) *LPS XLVII*, Abs. #2315. [10] Yakovlev O. I. et al. (2017) *Geochem. Int.* 55, 3, 251–256. [11] Krot A. N. et al. (2009) *GCA* 73, 4963–4997.